JOURNAL OF APPLIED CRYSTALLOGRAPHY

Volume 54 (2021)

**Supporting information for article:**

# *In situ* energy-dispersive X-ray diffraction of local phase dynamics during solvothermal growth of Cu4O3

**Zhelong Jiang, Jai Sharma, John S. Okasinski, Haiyan Chen and Daniel P. Shoemaker**

# In situ energy-dispersive X-ray diffraction of local phase dynamics during solvothermal growth of $Cu_4O_3$

## Supporting Information

Zhelong Jiang,[*a†] Jai Sharma,[a] John S. Okasinski,[b] Haiyan Chen,[c] and Daniel P. Shoemaker[*a]

[a] *Department of Materials Science and Engineering, Frederick Seitz Materials Research Laboratory, University of Illinois at Urbana-Champaign, Urbana, Illinois 61801, USA.*

[b] *X-ray Science Division, Advanced Photon Source, Argonne National Laboratory, Lemont, Illinois 60439, USA*

[c] *Mineral Physics Institute, Stony Brook University, Stony Brook, New York 11794, USA*

[†] *Current affiliation: SSRL Materials Science Division, SLAC National Accelerator Laboratory, Menlo Park, California 94025, USA*

[*] *e-mail: zjiang18@slac.stanford.edu; dpshoema@illinois.edu*

## Data Conversion

EDXRD data recorded at APS 6-BM-B were converted by Plot85 to yield data of interplanar spacing (d) *vs.* intensity (DvsI) for each detector element. A custom script was used to convert the d-spacing into $2\theta$ values as would be recorded using a monochromatic Mo-$K_{\alpha 1}$ X-ray wavelength using Bragg's law $2d\sin\theta = \lambda$, where $\lambda = 0.7093$ Å and $\theta = 3.25^\circ$. This generated the equivalent $2\theta$ *vs.* intensity ($2\theta$vsI) data for each detector element.

DvsI and $2\theta$vsI data for the entire detector were obtained by binning the combined data from the 10 individual detector elements using custom scripts. This was done because the registered values of d within each detector element were irregularly spaced, and because different values of d were registered by different detector elements. Average X-ray intensity from registered d (or $2\theta$) values within a predefined bin interval was calculated and stored against the middle value of the d (or $2\theta$) bin. The bin size used for DvsI data was 0.005 Å, and the bin size used for $2\theta$vsI data was $0.05^\circ$.

## Peak fitting

Peak fitting was performed on the binned $2\theta$vsI data using TOPAS 5.

The CuO (111) peak has partial overlap with a large peak contributed by $Cu_4O_3$ (202) and (004), $Cu_20$ (111) and CuO ($1\bar{1}\bar{1}$). Because the intensities from $Cu_4O_3$ (202) and $Cu_2O$ (111) dominate the large peak, we deconvoluted this overall peak as two individual peaks. Together with CuO (111), the $2\theta$ range of 14.8–18.3° was fitted by three pseudo-voigt peaks, representing contributions from $Cu_4O_3$ (202) (centered around 16.25°), $Cu_2O$ (111) (centered around 16.47°), and CuO (111) (centered around 17.55°). The fitted areas of $Cu_4O_3$ (202) and $Cu_2O$ (111) are found to be interdependent, thus they are unreliable and not discussed. The values and uncertainties of fitted CuO (111) by TOPAS were extracted.

$Cu_2O$ (200) has partial overlap with $Cu_4O_3$ (220). Therefore, the $2\theta$ range of 18.2–21.0° was fitted by two pseudo-voigt peaks, representing contributions from $Cu_2O$ (200) (centered around 19.22°) and $Cu_4O_3$ (220) (centered around 19.84°). The fitted values and uncertainties were extracted for both peaks.

$Cu_2O$ (224) was fitted by a split-pseudo-voigt peak in the $2\theta$ range of 24.8–26.6°. $Cu_2O$ (224) peak center is around 25.91°.

## Discussion of powder diffraction intensity

The classical expression for the integrated intensity of a diffraction peak from randomly distributed powder in transmission geometry is given by equation 1: [1]

$$P = \left(\frac{e^4}{8\pi m_e^2 c^4}\right)\left(\frac{I_0\lambda^3}{R}\right)(LP)\left(\frac{mF_T^2}{v_n^2}\right)V \tag{1}$$

where $P$ is the integrated intensity, the terms in the first bracket is a constant of fundamental quantities ($e$ is elementary charge, $m_e$ is electron mass, and $c$ is speed of light), the second term depends on the measurement setup ($I_0$ is the incident X-ray intensity, $\lambda$ is X-ray wavelength, and $R$ is the sample-to-detector distance), LP is the Lorentzian-polarization factor ($LP = \frac{1}{\sin\theta\sin 2\theta}$ for vertical scattering plane synchrotron beam, and $LP = \frac{1+\cos^2 2\theta}{2\sin\theta\sin 2\theta}$ for unpolarized beam), the term in the fourth bracket depend on the crystal structure of the material ($m$ is multiplicity, $F_T^2$ is structure factor squared, and $v_n$ is the unit cell volume), and $V$ is the volume of the crystal in the beam.

For normal XRD, scattered intensity is recorded against $2\theta$ so equation 1 (for synchrotron scattering) can be re-arranged as follows to show $\theta$ dependence:

$$P(\theta) = \left(\frac{e^4}{8\pi m_e^2 c^4}\right)\left(\frac{I_0\lambda^3}{R}\right)\left(\frac{1}{\sin\theta\sin 2\theta}\right)\left(\frac{mF_T^2(q)}{v_n^2}\right)V \tag{2}$$

where structure factor $F_T$ is dependent on the length of scattering vector $q = \frac{4\pi\sin\theta}{\lambda}$. This is the equation that Rietveld refinement is based on. Quantitative Rietveld refinement derives sample quantity $V$ from the measured $P(\theta)$ based on structure model.

For EDXRD, scatterd intensity is recorded against $\lambda$ so equation 1 can be re-arranged as follows to show $\lambda$ dependence:

$$P(\lambda) = \left(\frac{e^4}{8\pi R m_e^2 c^4}\right)\left(\frac{1}{\sin\theta\sin 2\theta}\right)(I_0(\lambda)\lambda^3)\left(\frac{mF_T^2(q)}{v_n^2}\right)V \tag{3}$$

where we have indicated the dependence of incident energy on wavelength, and again $F_T$ has some $\theta$ dependence through scattering vector $q$.

The structure factor $F_T(q)$ has both $\theta$ and $\lambda$ dependence, but its value for one peak is going to be the same in both normal XRD and EDXRD due to its ultimate $q$ dependence. However, for quantitative analysis, one important difference can be seen by comparing equation 2 and equation 3. For different peaks in normal XRD, the $I_0$ and $\lambda$ causing diffraction are the same, and the peak intensities are altered by the LP factor. But in EDXRD, LP factor is a constant, but for different peaks, the recorded $\lambda$ causing diffraction is different,

and so is $I_0$.

Because of this difference, even though $\lambda$ values in EDXRD can be converted into equivalent $2\theta$ in XRD, the dependence of intensity on converted $2\theta$ do not have the same mathematical expression. Most Rietveld refinement algorithms were written based on equation 2 for quantitative analysis and therefore are not suitable to use with quantitative analysis of EDXRD data. Furthermore, we did not obtain precise measurement of $I_0$ variation with $\lambda$.

## References

1 B. E. Warren, *X-ray diffraction*, Dover Publications, Reprint edn, 1990.

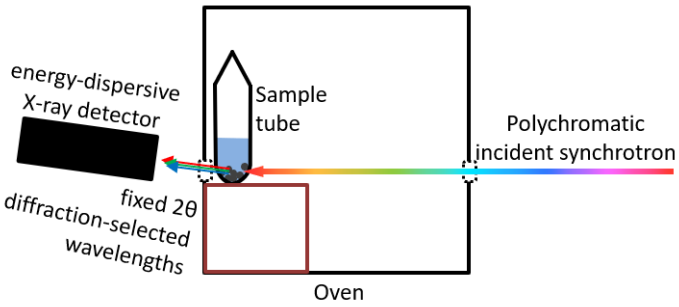


Figure S1 Schematic drawing of the EDXRD setup used in this study.

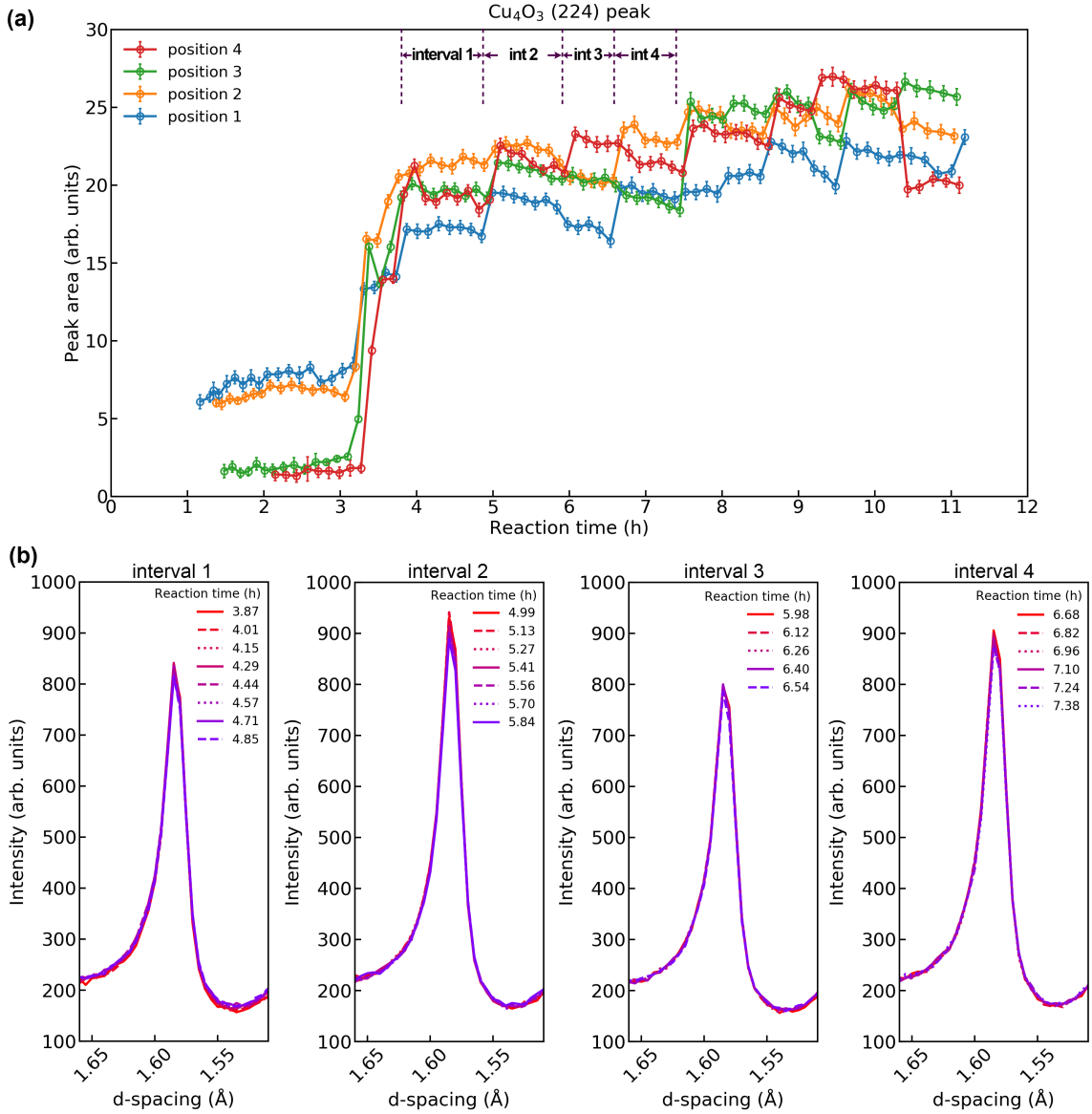


Figure S2 (a) Changes in the fitted $Cu_4O_3$ (224) peak area with reaction time for four positions during in situ EDXRD investigation. (b) Direct visualizations of the $Cu_4O_3$ (224) peak at position 1 during the time intervals indicated in (a).

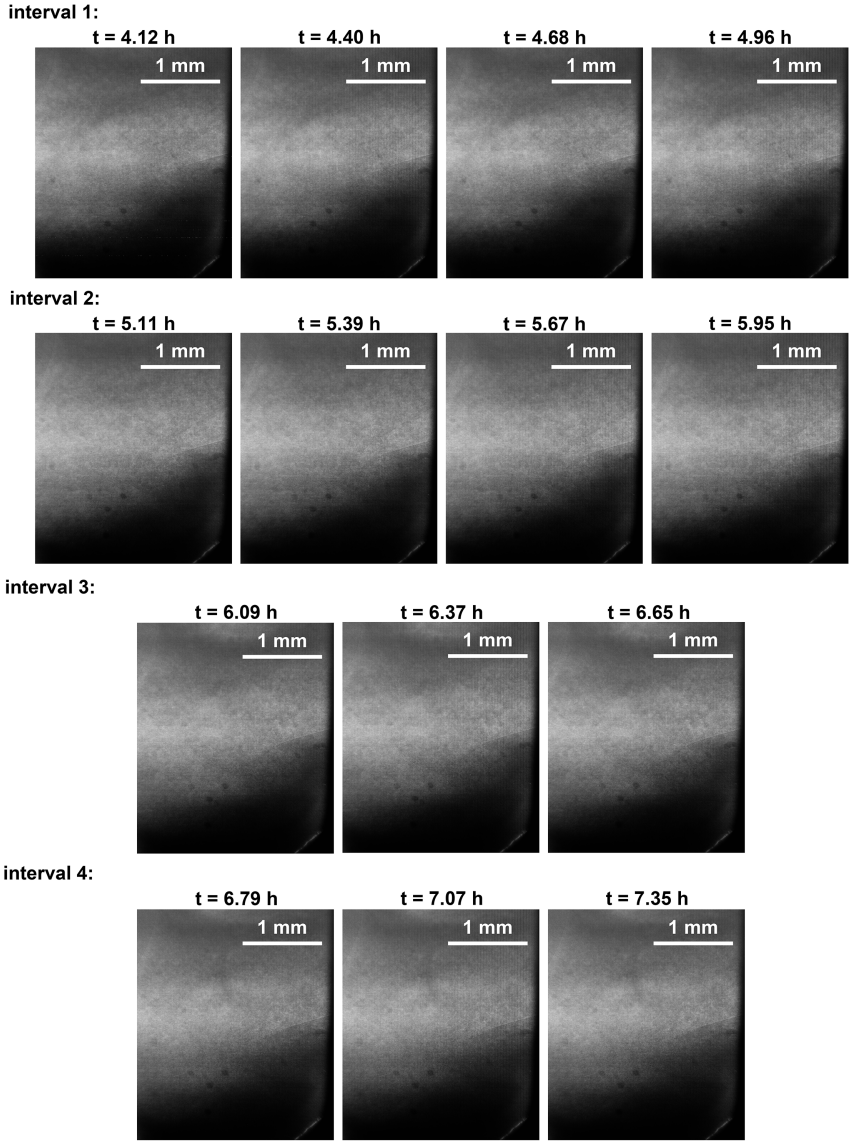


Figure S3 Some radiography images taken during different time intervals discussed in the main article. Radiography images within each interval have no discernible differences. However, some changes can be seen in the images from different intervals due to physical redistribution of the powders caused by bubble formation.

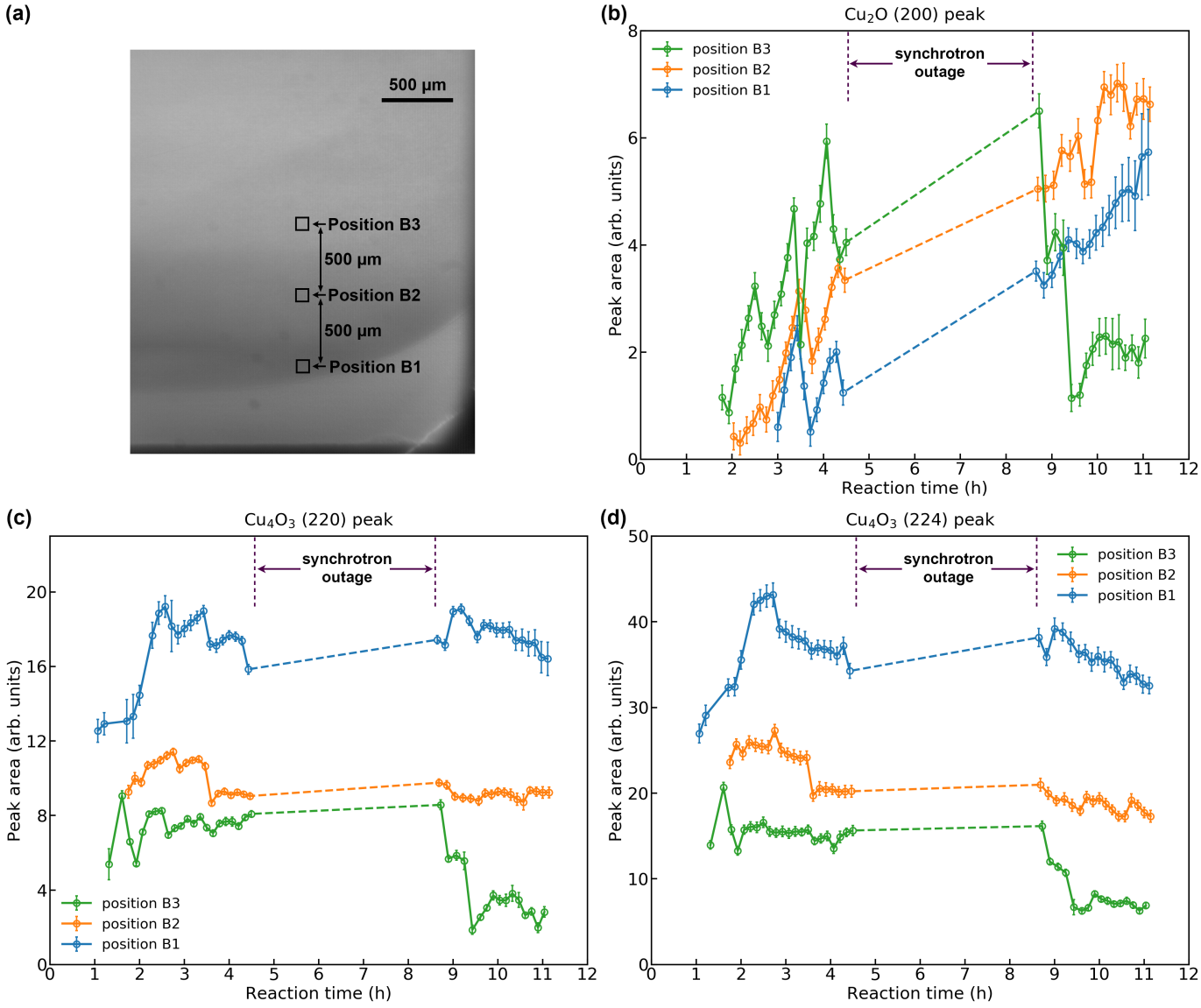


Figure S4 In situ EDXRD was performed for a different sample tube. (a) A radiography image showing the positions where in situ EDXRD signals were collected. The positions are 500 µm apart vertically. Results of the fitted (b) $Cu_2O$ (200), (c) $Cu_4O_3$ (220), and (d) $Cu_4O_3$ (224) peak areas during in situ EDXRD for these positions. There was a synchrotron outage during the middle of this investigation, whose duration is shown with dashed lines.

This sample had solvent composed of 33 vol% DMF and 67 vol% ethanol in contrast to the 20 vol% DMF sample discussed elsewhere. This small change of solvent composition has some effect on the balance between the precipitation phases but no change on the solvothermal reaction mechanisms. Because of having more reducing agent DMF, the amount of CuO formed in this sample was too small for CuO (111) to be reliably fitted, so it is not shown. The long-term changes during active in situ EDXRD periods have comparable trends with that during the period without X-rays.